

## Nusselt Number Correlation of SAH

Foued Chabane<sup>\*,a,b</sup>, Nouredine Moummi<sup>a,b</sup>, Said Benramache<sup>c</sup>, Okba Belahssan<sup>c</sup>, Djamel Bensahal<sup>a</sup>

<sup>a</sup>Mechanical Department, Faculty of Technology  
University of Biskra 07000, Algeria

<sup>b</sup>Mechanical Laboratory, Faculty of Technology  
University of Biskra 07000, Algeria

<sup>c</sup>Material Sciences Laboratory, Faculty of Science  
University of Biskra 07000, Algeria

### Abstract

This paper presents the experimentally investigated thermal performance of a single pass solar air heater. The effects of mass flow rate of air on the outlet temperature, Nusselt Number, Reynolds Number, Prandtl Number, heat transfer in the thickness of the solar collector and thermal efficiency were studied. Experiments were performed for the mass flow rates of 0.0108, 0.0145 and 0.0184 kg/s. For this effect was have created a new correlation correspondent of solar air collector without using fins was created it was written and expressed as  $Nu = \kappa_1 \times Re^{0.939} Pr^{0.523} \exp(1.2 \times m) \times h^{[0.0505 \times Pr]}$ . The maximum efficiency levels obtained for the 0.0108, 0.0145 and 0.0184 kg/s were 28.63, 39.69 and 55.69% respectively. A comparison of the results of the solar collector without fins shows a substantial enhancement in thermal efficiency.

**Keywords:** Correlation, Solar air collector, Heat transfer, Design, Temperature, Nusselt number

### 1. Introduction

This paper presents an experimental analysis of a single pass solar air collector without using fins. A comparison of results reveals that the thermal efficiency of a single pass solar air collector as a function of mass flow rate is higher with increased flow rate. On the other hand, several configurations of absorber plates have been designed to improve the heat transfer coefficient. Increasing the absorber area or fluid flow heat-transfer area will increase the heat transfer to the flowing air, on the other hand, will increase

the pressure drop in the collector, thereby increasing the required power consumption to pump the air flow crossing the collector [1, 2]. Artificial roughness obstacles and baffles in various shapes and arrangements were employed to increase the area of the absorber plate. As a result, the heat transfer coefficient between the absorber plate and the air pass is improved [3]. This paper reports on experimental investigation of the thermal performance of a single and double pass solar air heater with fins attached and a steel wire mesh as absorber plate [4].

The flat-plate solar air heater [5–8] is considered to be a simple device consisting of one or more glass (or transparent) covers situated above an absorbing plate with the air flowing over [7, 8], under [5–7] or simultaneously over and under [9] the absorbing plate. The conventional flat-plate solar air heater was investigated for heat-transfer efficiency improve-

\*Corresponding author

Email addresses: fouedmeca@hotmail.fr (Foued Chabane<sup>\*,a</sup>), nmoummi@lgm-ubiskra.net (Nouredine Moummi<sup>a</sup>), benramache.said@gmail.com (Said Benramache), bel\_okba@yahoo.fr (Okba Belahssan), bensahal.dz@gmail.com (Djamel Bensahal)

ment by introducing free convection [10] forced convection [11, 12] extended heat-transfer area [13, 14] and increased air turbulence [15, 16]. Moreover, the adoption of the recycle-effect concept can effectively enhance the heat transfer rate and has been applied in many separation processes and reactor design, as confirmed by previous works [17–21].

The effects of the flow ratio of air mass flow rate on the heat transfer rate, heat-transfer efficiency improvement, and the power consumption increment are also delineated. The bed heights were 7 cm and 3 cm for the lower and upper channels respectively. The predictions are done at air mass flow rates ranging between 0.02 and 0.1 kg/s. The fins serve as heat transfer augmentation features in solar air heaters, but they increase the pressure drop in flow channels. Results indicate that the high efficiency of the optimized fin improves the heat absorption and dissipation potential of a solar air heater [22]. A double flow solar air heater was designed with fins attached over and under the absorbing plate. This resulted in a considerable improvement in the collector efficiency of double flow solar air heaters with fins compared to single flow operating at the same flow rate [23]. The effect of the mass flow rate between 0.012 and 0.016 kg/s on the solar collector with longitudinal fins as reported in [24–34]. Many investigations on forced convective heat transfer in smooth and roughened ducts have been reported in the literature. Artificial roughness on the surface of absorber plate can be provided by fixing small diameter wires, ribs formed by machining process, wire mesh or expanded metal mesh and by forming dimple/protrusion shape geometry as was reported by Bhushan and Singh [35], and Varun et al. [36]. Experimental investigations on heat transfer and friction in artificially roughened solar air heater ducts were reported by Gupta et al. [37], Jaurker et al. [38], Karwa [39], Karmare and Tikekar [40], Momin et al. [41], and Saini and Saini [42]. The Nusselt number and friction factor correlations were developed by these investigators using experimental data.

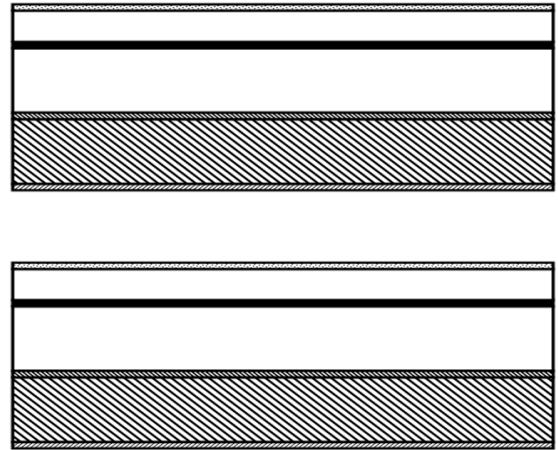


Figure 1: Composition of a solar box without fins

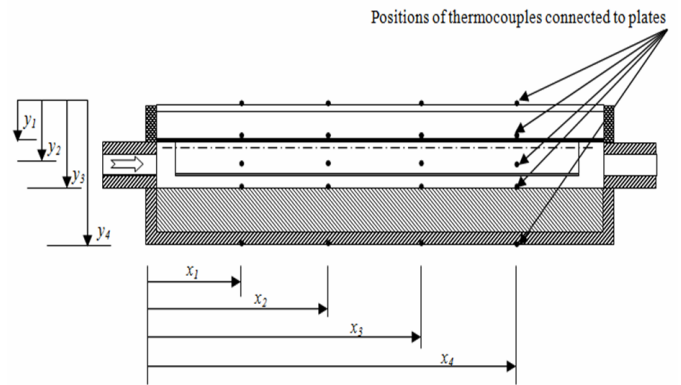


Figure 2: Air heater sections and locations of the measuring parameters

## 2. Experimental

### 2.1. Description of the solar air heater considered in this work

A schematic view of the constructed single-flow under an absorber plate is shown in Fig. 1, and photographs of the two different absorber plates of the collectors and a view of the absorber plate in the collector box are shown in Fig. 2, respectively. In this study, two modes of absorber plates were used. The absorbers were made of galvanized iron sheet with black chrome selective coating. The dimension and plate thickness for the solar collector were 0.5 mm. Plexiglas of 3 mm thickness was used as glazing. A single transparent cover was used in both collectors.

Thermal losses through the collector backs are mainly due to conduction across the insulation

(thickness 4 cm), whereas losses caused by wind and thermal radiation of the insulation are assumed to be negligible. After installation, the collectors were left operating for several days under normal weather conditions for weathering processes.

Thermocouples were positioned evenly, on the top surface of the absorber plates, at identical positions along the direction of flow, for both collectors. Inlet and outlet air temperatures were measured by two well insulated thermocouples. The output from the thermo-couples was recorded in degrees Celsius by means of a digital thermocouple thermometer DM6802B: measurement range  $-50^{\circ}\text{C}$  to  $1300^{\circ}\text{C}$  ( $-58^{\circ}\text{F}$  to  $1999^{\circ}\text{F}$ ), resolution:  $1^{\circ}\text{C}$  or  $1^{\circ}\text{F}$ , accuracy:  $\pm 2.2^{\circ}\text{C}$  or  $\pm 0.75\%$  of reading and Non-Contact digital infrared thermometer temperature laser gun model number: TM330: accuracy  $\pm 1.5\text{C}/\pm 1.5\%$ , measurement range  $-50^{\circ}\text{C}$  to  $330^{\circ}\text{C}$  ( $-58^{\circ}\text{F}$  to  $626^{\circ}\text{F}$ ) resolution  $0.1^{\circ}\text{C}$  or  $0.1^{\circ}\text{F}$ , emissivity 0.95. The ambient temperature was measured by a digital thermometer with sensor in display LCD CCTV-PM0143 placed in a special container behind the collectors' body. The total solar radiation incident on the surface of the collector was measured with a Kipp and Zonen CMP 3 Pyran-ometer. This meter was placed adjacent to the glazing cover, at the same plane, facing due south. The measured variables were recorded at time intervals of 15 min and include: insolation, inlet and outlet temperatures of the working fluid circulating through the collectors, ambient temperature, absorber plate temperatures at several selected locations and air flow rates (Lutron AM-4206M digital anemometer). All tests began at 9 AM and ended at 4 PM.

The layout of the solar air collector studied is shown in Figs. 1, 2. Collector A served as the baseline, with the following parameters:

- The solar collecting area was 2 m (length)  $\times$  1 m (width);
- The installation angle of the collector was  $45^{\circ}$  from the horizontal;
- Height of the stagnant air layer was 0.02 m;
- Thermal insulation board EPS (expanded polystyrene board), with thermal conductivity

$0.037\text{ W}/(\text{m K})$ , was put on the exterior surfaces of the back and side plates, with a thickness of 40 mm.

- The absorber was of a plate absorption coefficient  $\alpha = 0.95$ , the transparent cover transmittance  $\tau = 0.9$  and absorption of the glass covers,  $\alpha_g = 0.05$ ;
- 20 positions of thermocouples connected to plates and two thermocouples to outlet and inlet flow Fig. 3.

### 3. Thermal analysis and uncertainty

#### 3.1. Heat transfer coefficients

The convective heat transfer coefficient  $h_w$  for air flowing over the outside surface of the glass cover depends primarily on the wind velocity  $V_{wind}$ . McAdams [43] obtained the experimental result as:

$$h_w = 5.7 + 3.8V_{wind} \quad (1)$$

where the units of  $h_w$  and  $V_{wind}$  are  $\text{W}/\text{m}^2\text{K}$  and  $\text{m}/\text{s}$ , respectively. An empirical equation for the loss coefficient from the top of the solar collector to the ambient was developed by Klein [44]. The heat transfer coefficient between the absorber plate and the airstream is always low, resulting in low thermal efficiency of the solar air heater. Increasing the area of the absorber plate shape will increase the heat transferred to the air.

#### 3.2. Collector Thermal Efficiency

The efficiency of a solar collector is defined as the ratio of the amount of useful heat collected to the total amount of solar radiation striking the collector surface during any period of time:

$$\eta = \frac{Q_u}{I_0 \times A_C} \quad (2)$$

The equation for mass flow rate ( $m$ ) is  $m = \rho \times Q$  where  $\rho$  is the density of air, which depends on the air temperature, and  $Q$  is the volume flow rate, which depends on the pressure difference at the orifice as measured from the inclined tube manometer and temperature.

Useful heat collected for an air-type solar collector can be expressed as:

$$Q_u = \dot{m}C_p(T_{out} - T_{in}) \quad (3)$$

where  $C_p$  is the specific heat of the air,  $A_c$  is the area of the collector. The fractional uncertainty about the efficiency from Eq. (3) is a function of  $\Delta T$ ,  $m$ , and  $I_0$ , considering  $C_p$  and  $A_c$  as constants.

$$\text{With } \dot{m} = V_f \cdot S$$

So, collector thermal efficiency becomes,

$$\eta = \dot{m}C_p \frac{(T_{out} - T_{in})}{I A_C} \quad (4)$$

Thermal properties of air are considered to be variables according to the following expressions (Tiwari, 2002), where the fluid temperature is evaluated in Celsius [45]:

$$C_p = 999.2 + 0.1434T_f + 1.101 \times 10^{-4}T_f^2 - 6.7581 \times 10^{-8}T_f^3 \quad (5)$$

$$\lambda = 0.0244 + 0.6773 \times 10^{-4}T_f \quad (6)$$

$$\mu = 0.0284 \times 10^{-4} + 0.00105 \times 10^{-4}T_f \quad (7)$$

Air density is calculated assuming the fluid is an ideal gas by the expression:

$$\rho = 353.44/T_f \quad (8)$$

where  $T_f$  is the absolute air temperature.

#### 4. Equations used for calculation

The following equations were used for calculating the mass flow rate of air,  $m$  (Saini and Saini, 1997), heat energy transfer,  $Q_u$ , heat transfer coefficient,  $h$  (Saini and Saini, 1997) [46].

$$m = Cd \left[ \frac{2\rho(\delta p_0)}{(1 - \beta^4)} \right]^{0.5} \quad (9)$$

$$h = \frac{Q_u}{A_c(T_p - T_f)} \quad (10)$$

where  $T_p$  and  $T_f$  are average values of absorber plate temperature and air temperature, respectively. The average temperature of the plate was determined from the temperature recorded at four different locations along the test section of the absorber plate, as shown in Fig. 3. It was found that the temperature of the absorber plate varies predominantly in the flow direction only and is linear. The air temperature was determined as an average of the temperatures measured at four central locations over the test length of the duct along the flow direction, as shown in Fig. 3. The Nusselt number was calculated using the following equation:

$$Nu = \frac{hD_h}{k} \quad (11)$$

The Prandtl number is a dimensionless number approximating the ratio of momentum diffusivity (kinematic viscosity) and thermal diffusivity and can be expressed:

$$Pr = \frac{C_p\mu}{\lambda_a} \quad (12)$$

#### 5. Discussion

Fig. 4 shows the average temperature distribution in the thickness of a solar collector, indicated the variation of the average temperature correspondent with the transparent cover, absorber plate, air, bottom plate and exterior plate. We can be seen the difference in Fig. 4; at the mass flow rates 0.0108, 0.0145 and 0.0184 kg/s, As discussed in the previous chapter, conventional SAH mainly consists of panels, insulated hot air ducts and air blowers in active systems, forming a passage for airflow. A plastic cover is fixed above the absorber plate and the system is thermally insulated from the back and on the sides. The following sections will discuss the new designed SAHs used in the experiments, the measurement devices, calibration process, and the experimental procedure.

Fig. 5 illustrates the variation of temperatures of absorber plate along the solar air heater. It may be remarked that the temperature of an absorber plate in general decreases along the air heater from  $x_1$  to  $x_2$  and increases evolutions from  $x_2$  to  $x_4$  about the mass flow rate 0.0108, 0.0145 and 0.0184 kg/s. The

experimental results indicated by measurement data illustrate that the maximum temperatures for an absorber plate are obtained at  $x_1$  and  $x_3$ . A cause for the reduction of temperature of the absorber plate from  $x_1$  to  $x_2$  may be that the air takes more heat from the absorber plate as shown in Fig.6 and to raise the temperature of the absorber plate again means the air loses heat or the air has insufficient time to stay and acquire heat.

Figure 6 shows the average temperature of a solar collector dependant fluid as a function of length, from 0.388 to 1.552 m, corresponding to flat-plate at mass flow rates 0.0108, 0.0145 and 0.0184 kg/s. As can be seen, the evolution of the curves takes an irregular, non-linear form; a decrease in the temperature of air from  $x_1$  to  $x_4$  results in an automatic increase in a regular fashion in maximum temperature registered in  $x_2$  and  $x_3$  : ( $T_f = 76.5, 78$  and  $75.5^\circ\text{C}$ ) and ( $T_f = 74, 76$  and  $72.25^\circ\text{C}$ ) at  $x = 0.776$  and  $1.164$  m respectively. This can be explained by the fluid taking more heat energy from the absorber plate and bottom plate: which is working as another surface of heat exchange with fluid; of  $x_2$  and  $x_3$  points and as a function of the length of the solar collector. Increasing the mass flow rate resulted in increasing the temperature of the air; this means that bringing the fluid takes more heat from the absorber plate and cools it. The evolution of curves corresponds to mass flow rates and average temperature  $T_f(x_1, m) < T_f(x_2, m) > T_f(x_3, m) > T_f(x_4, m)$ .

### 5.1. Development of correlations for the Nusselt number

Based on the experimental study, the effect of various parameters on the Nusselt number was discussed earlier and is reproduced as follows: the Nusselt number increases monotonically as the Reynolds number increases ( $Re$ ).

The Nusselt number is strongly dependent on the Prandtl number, specific heat of air (J/kg K), density, temperature of air and the operating parameter ( $Re$ ). Thus the equation for the Nusselt number can be written as

$$Nu = f(Re, Pr, \rho, T_f, h, C_p, m) \quad (13)$$

$$Nu = \kappa_1 \times Re^n Pr^j \exp(a \times m) \times h^{[b \times Pr]}$$

Data was collected from the experimental study for temperature of air and plate, manometer reading across the orifice for calculating air mass flow rate to calculate the heat transfer coefficient. The Nusselt number calculated using the heat transfer coefficient was plotted against the Reynolds number. Regression analysis was performed to fit a straight line through the data point, resulting in the following:

$$\chi_1 = 0.0318 \quad (14)$$

$$Nu = \chi_1 \times Re^{0.939} \quad (15)$$

The constant  $\chi_1$  is dependent of the parameters  $Pr$  and  $m$ . The relative Prandtl number ( $Pr$ ) is incorporated to show the effect of the Prandtl Number on the Nusselt number. The values of  $Nu / (Re^{0.939})$ , respectively, are plotted against the relative Prandtl number  $Pr$  as shown in Fig. 7. Now, regression analysis was carried out to fit a straight line through these points, and prepared as follows:

$$\zeta_1 = 0.0543 \quad (16)$$

$$Nu = \zeta_1 \times Re^{0.939} Pr^{0.523} \quad (17)$$

The constants is the function of the remaining parameter, relative mass flow rate, this parameter is incorporated and the values of  $Nu / (Re^{0.939} (Pr)^{0.523})$ , respectively, are plotted against the values of  $m$ , as shown in Fig. 8. The best fit regression results in the following correlation for the Nusselt number:

$$\psi_1 = 0.0531 \quad (18)$$

$$Nu = \psi_1 \times Re^{0.939} Pr^{0.523} \exp(1.2 \times m) \quad (19)$$

The constant is the function of the remaining parameter, the relative heat transfer coefficient; this parameter is incorporated and the values of  $Nu / (Re^{0.939} (Pr)^{0.523} \exp(1.2m))$  are plotted against the values of  $h$ , as shown in Fig. 9. The best fit regression results in the following correlation for the Nusselt number:

$$\kappa_1 = 0.0505 \quad (20)$$

Table 1: Constants data of the Nusselt number for solar collector, corresponding to the mass flow rates of 0.0108, 0.0145 and 0.0184 kg/s, with tilt angle  $\beta = 45^\circ$

	1	2	3	4
	$Nu = A \times Re^n Pr^j \exp(a \times m) \times h^{[b \times Pr]}$			
A	0.0318	0.0543	0.0531	0.0505
n	0.939	0	0	0
j	0.939	0.523	0	0
a	0.939	0.523	1.2	0
b	0.939	0.523	1.2	0.0505

$$Nu = \kappa_1 \times Re^{0.939} Pr^{0.523} \exp(1.2 \times m) \times h^{[0.0505 \times Pr]} \quad (21)$$

Figure 10 is a sample figure illustrating the Reynolds number variation of the Nusselt number for different values of correlation. It may be remarked from Fig. 7 that the maximum value of the Nusselt number occurs at the entry section of the air heater, which is mostly affected by heat transfer from the wall and the inside circumference of the air heater. Further, it may be concluded that the heat transfer decreases as solar radiation increases. Increasing solar radiation leads to increases in the temperature of the absorber plate and of the near wall air and, consequently, to an increase in air viscosity. This increase in air viscosity affects the wall shear stress and decreases the local  $Re$  as well, which causes an increase in thermal boundary layer thickness resulting in a decrease in the convective heat transfer coefficient. These match the findings presented in [19]. Five curves for the Nusselt number can be seen: one experimental, other correlations as a function of the Reynolds number, the Prandtl number, mass flow rate and heat transfer coefficient.

Fig. 11 shows the variation of thermal efficiency and solar intensity with air mass flow rates. The thermal efficiency used to evaluate the performance of the solar air heater was calculated; it is found from the figure that thermal efficiency increases with increasing solar intensity and mass flow rates as a function of time. The efficiencies of the flat plate collector with  $m = 0.0203$  kg/s are higher than those of the collector with mass flow rates less than 0.0203 kg/s Fig. 11 shows a comparison of thermal efficiency for

Table 2: Experimental data for flat-plate, corresponding thermal efficiency and solar intensity of solar collector at mass flow rates of 0.0108 to 0.0203 kg/s, on 24 and 25/01/2012, and 01, 19 and 27/02/2012, respectively

$m$ , kg/s	$I$ , W/m <sup>2</sup>	$\eta$ , %	$T_{out}$ , °C	$T_{in}$ , °C
0.0108	733.00	28.63	48.15	23.00
0.0145	787.50	39.69	50.90	23.00
0.0161	793.00	46.98	54.05	24.10
0.0184	804.00	55.69	56.30	24.80
0.0203	823.50	63.61	58.70	25.30

the different mass flow rates of the solar collector. The results data of each solar air heater are shown in Table 2. It can be seen that the mean highest thermal efficiency ( $\eta = 63.61\%$ ) at solar intensity  $I = 823.50$  W/m<sup>2</sup> was obtained with air flow rate of 0.0203 kg/s 45° tilt angle at inlet temperature  $T_{in} = 25.30^\circ\text{C}$  and outlet temperature  $T_{out} = 58.70^\circ\text{C}$ . The mean lowest thermal efficiency ( $\eta = 28.63\%$ ) at solar intensity  $I = 733$  W/m<sup>2</sup> was obtained with an air flow rate of 0.0108 kg/s, 45° tilt angle at inlet temperature  $T_{in} = 23^\circ\text{C}$  and outlet temperature  $T_{out} = 48.15^\circ\text{C}$ . This indicates that the experimental efficiency of the collector increases as mass flow rates increase.

## 6. Conclusion

The following conclusions were drawn from experimental investigation of the solar air heater without fins: the Nusselt number increases as the Reynolds number increases. The maximum enhancement of the Nusselt number was found to be 56.39 at mass flow rate 0.0184 kg/s, which was better than for 0.0108 and 0.014 kg/s. Based on the experimental values, correlations for the Nusselt number were developed. Good agreement was found between the calculated and experimental values.

### Acknowledgments

The authors would like to thank Pr. H. Ben Moussa, Pr. S. Youcef-Ali and Dr. A. Brima for their helpful advice.

## References

- [1] E. K. Akpınar, F. Koçyigit, Experimental investigation of thermal performance of solar air heater having differ-

- ent obstacles on absorber plates, *Int Commun Heat Mass* 37 (4) (2010) 416–421.
- [2] S. Karsli, Performance analysis of new-design solar air collectors for drying applications, *Renewable Energy* 32 (10) (2007) 1645–1660. doi:10.1016/j.renene.2006.08.005.
- [3] B. S. Romdhane, The air solar collectors: Comparative study, introduction of baffles to favor the heat transfer, *Solar Energy* 81 (1) (2007) 139–149. doi:10.1016/j.solener.2006.05.002.
- [4] A. Omojaro, L. Aldabbagh, Experimental performance of single and double pass solar air heater with fins and steel wire mesh as absorber, *Applied Energy* 87 (12) (2010) 3759–3765. doi:10.1016/j.apenergy.2010.06.020.
- [5] D. J. Close, R. V. Dunkle, Behaviour of adsorbent energy storage beds, *Sol. Energy* 18 (4) (1976) 287–292.
- [6] C. H. Liu, E. M. Sparrow, Convective-radiative interaction a parallel plate channel-application to air-operated solar collectors, *Int. J. Heat Mass Transf.* 23 (8) (1980) 1137–1146.
- [7] M. K. Seluck, *Solar air heaters and their applications*, Academic Press, New York, 1977.
- [8] H. M. Tan, W. W. S. Charters, Experimental investigation of forced-convective heat transfer for fully-developed turbulent flow in a rectangular duct with asymmetric heating, *Sol. Energy* 13 (1) (1970) 121–125.
- [9] A. Whillier, Plastic covers for solar collectors, *Sol. Energy* 7 (3) (1963) 148–154.
- [10] H.-M. Yeh, C.-D. Ho, J.-Z. Hou, Collector efficiency of double-flow solar air heaters with fins attached, *Energy* 27 (8) (2002) 715–727. doi:10.1016/S0360-5442(02)00010-5.
- [11] F. Kreith, J. F. Kreider, *Principles of solar engineering*, 2nd Edition, McGraw-Hill, New York, 1978.
- [12] J. A. Duffie, W. A. Beckman, *Solar engineering of thermal processes*, 3rd Edition, Wiley, New York, 1980.
- [13] J. K. Tonui, Y. Tripanagnostopoulos, Improved pv/t solar collectors with heat extraction by forced or natural air circulation, *Renew. Energy* 32 (4) (2007) 623–637.
- [14] W. Gao, W. Lin, T. Liu, C. Xia, Analytical and experimental studies on the thermal performance of cross-corrugated and flat-plate solar air heaters, *Applied Energy* 84 (4) (2007) 425–441. doi:10.1016/j.apenergy.2006.02.005.
- [15] A. A. Mohamad, High efficiency solar air heater, *Sol. Energy* 60 (2) (1997) 71–76.
- [16] S. K. Verma, B. N. Prasad, Investigation for the optimal thermohydraulic performance of artificially roughened solar air heaters, *Renew. Energy* 20 (1) (2000) 19–36.
- [17] H. M. Yeh, Theory of baffled solar air heaters, *Energy* 17 (7) (1992) 697–702.
- [18] H. P. Garg, V. K. Sharma, A. K. Bhargava, Theory of multiple-pass solar air heaters, *Energy* 10 (5) (1985) 589–599.
- [19] C. D. Ho, W. Y. Yang, An analytical study of heat-transfer efficiency in laminar counter flow concentric circular tubes with external refluxes, *Chem. Eng. Sci.* 58 (7) (2003) 1235–1250.
- [20] C. Ho, C. Yeh, S. Hsieh, Improvement in device performance of multi-pass flat-plate solar air heaters with external recycle, *Renewable Energy* 30 (10) (2005) 1601–1621. doi:10.1016/j.renene.2004.11.009.
- [21] C. D. Ho, H. M. Yeh, S. C. Chiang, Mass-transfer enhancement in double-pass mass exchangers 348 with external refluxes, *Ind. Eng. Chem. Res.* 40 (24) (2001) 5839–5846.
- [22] P. N. Nwachukwu, Employing exergy-optimized pin fins in the design of an absorber in a solar air heater, *Energy* 35 (2) (2010) 571–575.
- [23] A. A. El-Sebaei, S. Aboul-Enein, M. R. I. Ramadan, S. M. Shalaby, B. M. Moharram, Thermal performance investigation of double pass-finned plate solar air heater, *Appl Energy* 88 (5) (2011) 1727–1739.
- [24] W. Lin, W. Gao, T. Liu, A parametric study on the thermal performance of cross-corrugated solar air collectors, *Appl Therm Eng* 26 (10) (2006) 1043–1053.
- [25] W. Gao, W. Lin, T. Liu, C. Xia, Analytical and experimental studies on the thermal performance of cross-corrugated and flat-plate solar air heaters, *Appl Energy* 84 (4) (2007) 425–441.
- [26] F. Chabane, N. Moumami, S. Benramache, Experimental analysis on thermal performance of a solar air collector with longitudinal fins in a region of biskra, algeria, *Journal of Power Technologies* 93 (1) (2013) 52–58.
- [27] F. Chabane, N. Moumami, S. Benramache, Performances of a single pass solar air collector with longitudinal fins inferior an absorber plate, *Am J Adv Sci Res* 1 (4) (2012) 146–157.
- [28] F. Chabane, N. Moumami, S. Benramache, Experimental study on heat transfer for a solar air heater and contribution the fins to improve the thermal efficiency, *Int J Adv Renew Energy Res* 487–494 (2012) 1.
- [29] F. Chabane, N. Moumami, S. Benramache, Experimental performance of solar air heater with internal fins inferior an absorber plate, in the region of biskra, *Int J Energ & Tech* 1–6 (2012) 4.
- [30] F. Chabane, N. Moumami, S. Benramache, Experimental study of heat transfer and thermal performance with longitudinal fins of solar air heater, *Journal of Advanced Research* doi:10.1016/j.jare.2013.03.001.
- [31] F. Chabane, N. Moumami, A. Brima, S. Benramache, Thermal efficiency analysis of a single-flow solar air heater with different mass flow rates in a smooth plate, *Frontiers in Heat and Mass Transfer* doi:10.5098/hmt.v4.1.3006.
- [32] F. Chabane, N. Moumami, S. Benramache, D. Bensahal, O. Belahssen, F. Z. Lemmadi, Thermal performance optimization of a flat plate solar air heater, *International Journal of Energy & Technology* 5 (8) (2013) 1–6.
- [33] F. Chabane, N. Moumami, S. Benramache, D. Bensahal, O. Belahssen, Effect of artificial roughness on heat transfer in a solar air heater, *Journal of Science and Engineer-*

- ing 1 (2) (2013) 85–93.
- [34] F. Chabane, N. Moumimi, S. Benramache, Design, developing and testing of a solar air collector experimental and review the system with longitudinal fins, International Journal of Environmental Engineering Research 2 (1) (2013) 18–26.
- [35] B. Bhushan, R. Singh, A review on methodology of artificial roughness used in duct of solar air heaters, Energy 35 (2010) 202–212.
- [36] Varun, R. Saini, S. Singal, A review on roughness geometry used in solar air heaters, Sol Energ 81 (11) (2007) 1340–1350.
- [37] D. Gupta, S. C. Solanki, J. S. Saini, Heat and fluid flow in rectangular solar air heater ducts having transverse rib roughness on absorber plates, Sol Energ 51 (1993) 31–37.
- [38] A. R. Jaurker, J. S. Saini, B. K. Gandhi, Heat transfer and friction characteristics of rectangular solar air heater duct using rib-grooved artificial roughness, Sol Energ 80 (2006) 895–907.
- [39] R. Karwa, Experimental studies of augmented heat transfer and friction in asymmetrically heated rectangular ducts with ribs on the heated wall in transverse, inclined, v-continuous and v-discrete pattern, Int Commun Heat & Mass Transfer 30 (2003) 241–250.
- [40] S. V. Karmare, A. N. Tikekar, Heat transfer and friction factor correlation for artificially roughened duct with metal grit ribs, Int J Heat & Mass Transfer 50 (2007) 4342–4351.
- [41] A. M. E. Momin, J. S. Saini, S. C. Solanki, Heat transfer and friction in solar air heater duct with v-shaped rib roughness on absorber plate, Int J Heat & Mass Transfer 45 (2002) 3383–3396.
- [42] R. P. Saini, J. S. Saini, Heat transfer and friction factor correlations for artificially roughened ducts with expanded metal mesh as roughness element, Int. J. Heat Mass Transfer 40 (4) (1997) 973–986.
- [43] W. McAdams, Heat Transmission, McGraw-Hill, New York, 1954.
- [44] E. Azad, Design, installation and operation of a solar thermal public bath in eastern iran, Energy for Sustainable Development 16 (1) (2012) 68–73. doi:10.1016/j.esd.2011.10.006.
- [45] G. N. Tiwari, Solar energy: fundamentals, design modeling and applications, CRC Press and Narosa Publishing House, New York and New Delhi, 2002.
- [46] R. P. Saini, J. S. Saini, Heat transfer and friction factor correlations for artificially roughened ducts with expanded metal mesh as roughness element, Int J Heat & Mass Transfer 40 (1997) 973–986.

## Nomenclature

- $\alpha_a$  Absorber plate absorption coefficient
- $\alpha_g$  Absorptivity of the glass covers

$\Delta T$	Temperature difference, °C
$\eta$	Collector efficiency,
$\kappa_1, \psi_1, \zeta_1, \chi_1$	Constants
$\tau$	Transparent cover transmittance
$\varepsilon$	Emissivity of absorber plate
$A_c$	Area of absorber plate surface, m <sup>2</sup>
$C_p$	Specific heat of air, J/(kg K)
$h$	Heat transfer coefficient, W/(m <sup>2</sup> °C)
$h_w$	Convection heat transfer coefficient, W/(m <sup>2</sup> K)
$I$	Global irradiance incident on solar air heater collector, W/m <sup>2</sup>
$m$	Air mass flow rate, kg/s
$Nu$	Nusselt number, -
$Pr$	Prandtl number, -
$Q$	Volume flow rate, m <sup>3</sup> /s
$Q_u$	Useful heat collected for an air-type solar collector, W
$Re$	Reynolds number, -
$S$	Passage cross section, m <sup>2</sup>
$t$	Time of the during day, hour
$T_{bp}$	Temperature of bottom plate, °C
$T_f$	Temperature of absorber plate, °C
$T_{in}$	Temperature inlet, °C
$T_{out}$	Outlet fluid temperature, °C
$T_P$	Temperature of absorber plate, °C
$V_f$	Air velocity, m/s <sup>2</sup>
$V_{wind}$	Wind velocity, m/s
$x_i$	Local direction longitudinal of points, m

- $y_i$  Local direction of thickness panel, m
- i Position of the thermocouple connected of 1 to 4

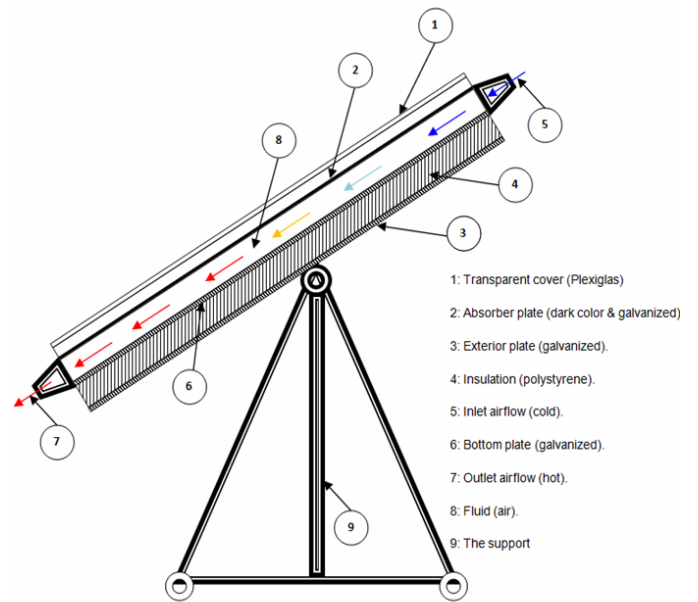


Figure 3: Schematic & photographic view of the solar air collector

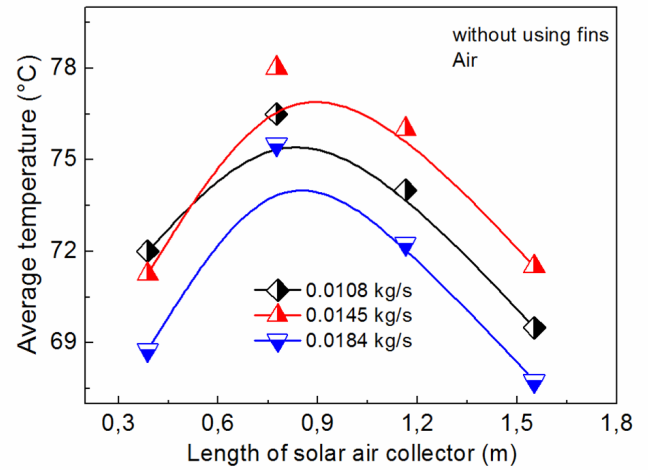
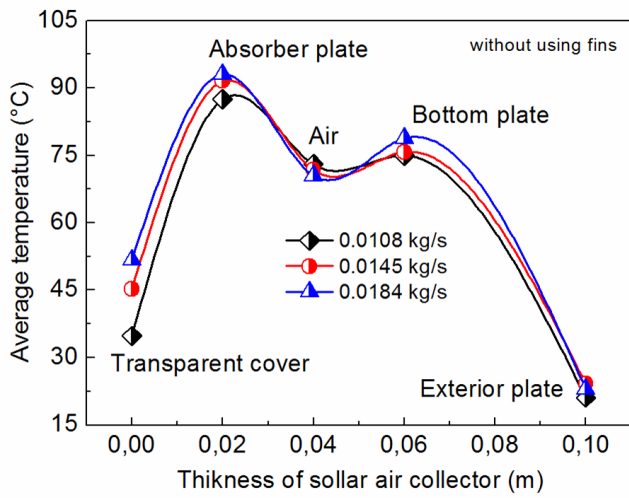


Figure 4: Average temperature in the thickness of a solar collector versus the whole area of the solar collector plates for a single pass solar air heater, with flow rates of 0.0108, 0.0145 and 0.0184 kg/s, for solar collectors without fins

Figure 6: Average temperature of air in the rectangular channel for a single pass solar air heater, with flow rates of 0.012, 0.014 and 0.016 kg/s, for solar collectors without fins

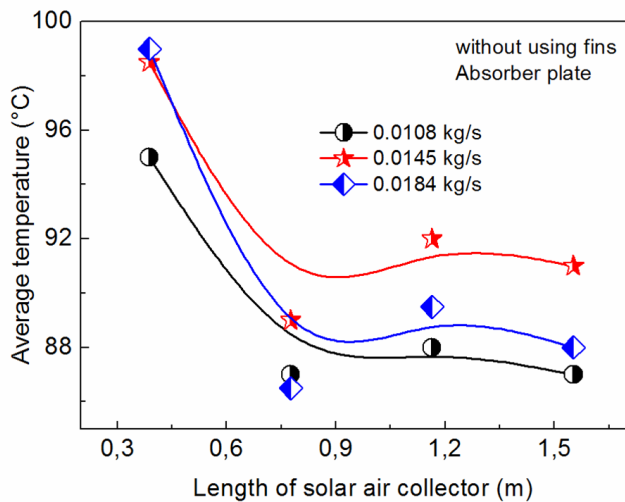


Figure 5: Average temperature of the absorber plate in the length of a solar collector for a single pass solar air heater, with flow rates of 0.0108, 0.0145 and 0.0184 kg/s, for solar collectors without fins

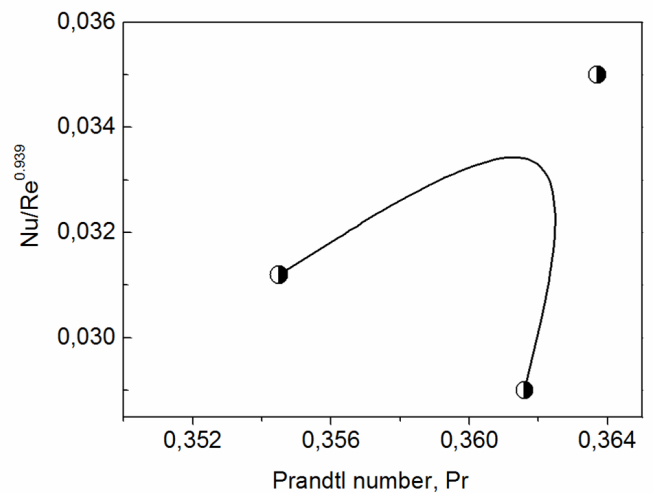


Figure 7:  $Nu/Re^{0.939}$ ; as a function of Prandtl number for solar collectors with and without using fins

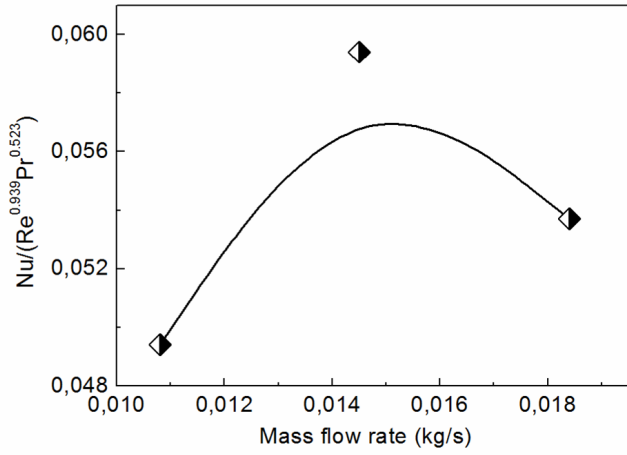


Figure 8:  $Nu/Re^{0.939}Pr^{0.523}$ ; as a function of mass flow rate for solar collectors with and without using fins

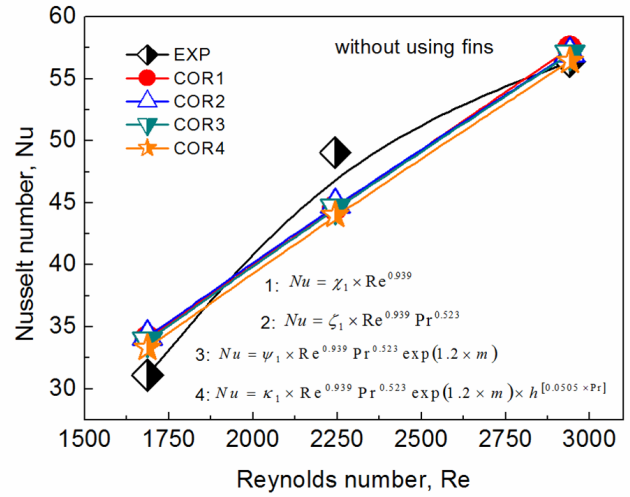


Figure 10: Nusselt number vs. Reynolds number

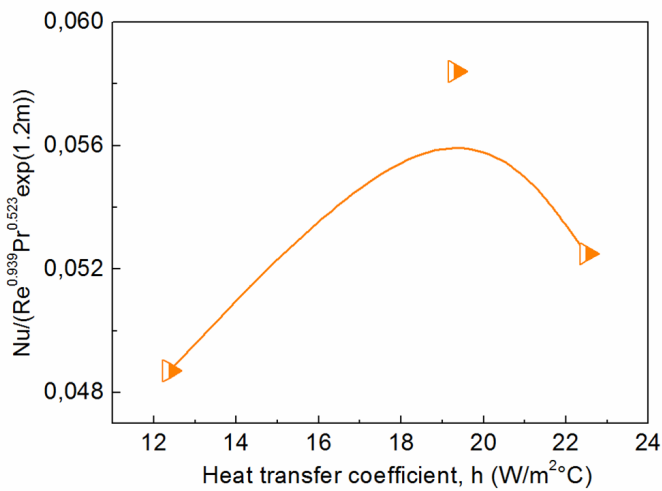


Figure 9:  $Nu/(Re^{0.939}Pr^{0.523} \exp(1.2m))$ ; as a function of heat transfer coefficient for solar collectors with and without using fins

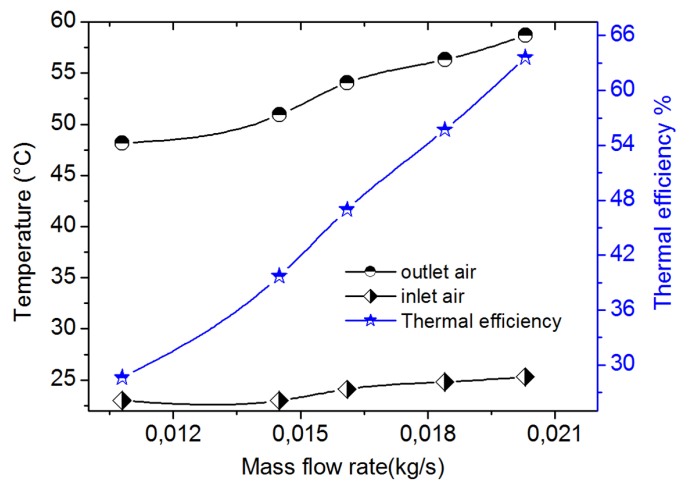


Figure 11: Outlet, inlet temperature and efficiency versus mass flow rate for single pass solar air heater